

NMR and Theoretical Study on the Coordination and Solution Structures of the Interaction between Diperoxovanadate Complexes and Histidine-like Ligands

Xian-Yong Yu, Shu-Hui Cai, Xin Xu,* and Zhong Chen*

Departments of Physics and Chemistry, State Key Laboratory of Physical Chemistry of Solid Surface, Xiamen University, Xiamen 361005, P.R. China

Received May 10, 2005

To simulate the types of coordination and solution structures of the active site of haloperoxidases, the interaction systems between diperoxovanadate complexes $[\text{OV}(\text{O}_2)_2\text{L}]^{n-}$ ($n = 1$ or 3 , $\text{L} = \text{oxalate}$ or H_2O) and a series of histidine-like ligands in solution have been studied by using 1D multinuclear (^1H , ^{13}C , and ^{51}V) NMR, 2D diffusion ordered spectroscopy, and variable-temperature NMR in 0.15 mol/L NaCl ionic medium, representing the physiological conditions of human blood. Some direct NMR data are given for the first time. The reactivity among the histidine-like ligands is imidazole > 2-methylimidazole > carnosine \approx 4-methylimidazole > histidine. Competitive coordination interactions result in a series of new peroxovanadate species $[\text{OV}(\text{O}_2)_2\text{L}']^-$ ($\text{L}' = \text{histidine-like ligands}$). When the ligands are 4-methylimidazole, histidine, and carnosine, a pair of isomers have been observed, which are attributed to different types of coordination between vanadium atom and ligands. The results of density functional theory calculations provided a reasonable explanation on the relative reactivity of the histidine-like ligands and the molar ratios of isomers. Theoretical results signify the importance of the solvation effect for the reactivity and stability of the interaction systems.

1. Introduction

Haloperoxidases is a class of enzymes which are able to oxidize halides in the presence of hydrogen peroxide to the corresponding hypohalous acids.^{1,2} The oxidized halogen species can halogenate selected organic compounds. Some of the haloperoxidases such as chloroperoxidase (V-CIPO) from *Curvularia inaequaliz* contain vanadium in the active site. Therefore, it is not surprising to see that the chemistry of vanadium-dependent haloperoxidases has recently encouraged many interests.^{3–24}

* To whom correspondence should be addressed. E-mail: chenz@jingxian.xmu.edu.cn (Z.C.); xinxu@xmu.edu.cn (X.X.).

- Messeschmidt, A.; Wever, R. *Proc. Natl. Acad. Sci.* **1996**, *93*, 392.
- Messeschmidt, A.; Prade, R.; Wever, R. *Biol. Chem.* **1997**, *378*, 309.
- Clague, M. J.; Keder, N. L.; Butler, A. *Inorg. Chem.* **1993**, *32*, 4754.
- Colpas, G. J.; Hamstra, B. H.; Kampf, J. W.; Pecoraro, V. L. *J. Am. Chem. Soc.* **1994**, *116*, 3627.
- Colpas, G. J.; Hamstra, B. H.; Kampf, J. W.; Pecoraro, V. L. *J. Am. Chem. Soc.* **1996**, *118*, 3469.
- Hamstra, B. J.; Colpas, G. J.; Pecoraro, V. L. *Inorg. Chem.* **1998**, *37*, 949.
- de la Rosa, R. I.; Clague, M. J.; Butler, A. *J. Am. Chem. Soc.* **1992**, *114*, 760.
- Conte, V.; Di Furia, F.; Moro, S. *Tetrahedron Lett.* **1994**, *35*, 7429.
- Andersson, M.; Conte, V.; Di Furia, F.; Moro, S. *Tetrahedron Lett.* **1995**, *36*, 2675.

It was reported that the peroxovanadate species, synthesized^{3–6} or generated in situ,^{7–10} provided a function that mimics the

- Conte, V.; Di Furia, F.; Moro, S.; Rabbolini, S. *J. Mol. Catal.* **1996**, *113*, 175.
- Crans, D. C.; Keramidas, A. D.; Hoover-Litty, H.; Anderson, O. P.; Miller, M. M.; Lemoine, L. M.; Pleasic-Williams S.; Vandenberg, M.; Rossomando, A. J.; Sweet, L. J. *J. Am. Chem. Soc.* **1997**, *119*, 5447.
- Cai, S. H.; Yu, X. Y.; Chen, Z.; Wan, H. L. *Chin. J. Chem.* **2003**, *21*, 746.
- Yu X. Y.; Cai, S. H.; Chen, Z.; Huang, P. Q. *Acta Chim. Sin.* **2003**, *61*, 994.
- Yu X. Y.; Cai, S. H.; Chen, Z. *Spectrochim. Acta A* **2004**, *60*, 391.
- Yu X. Y.; Cai, S. H.; Chen, Z. *Chin. J. Struct. Chem.* **2004**, *23*, 511.
- Schmidt, H.; Andersson, I.; Rehder, D.; Pettersson, L. *J. Inorg. Biochem.* **2000**, *80*, 149.
- Schmidt, H.; Andersson, I.; Rehder, D.; Pettersson, L. *Chem. Eur. J.* **2001**, *7*, 251.
- Gorzsas, A.; Andersson, I.; Schmidt, H.; Rehder, D.; Pettersson, L. *Dalton Trans.* **2003**, 1161.
- Gorzsas, A.; Andersson, I.; Pettersson, L. *Dalton Trans.* **2003**, 2503.
- Pettersson, L.; Andersson, I.; Gorzsas, A. *Coord. Chem. Rev.* **2003**, *237*, 77.
- Bortolini, O.; Carraro, M.; Conte, V.; Moro, S. *Eur. J. Inorg. Chem.* **1999**, 1489.
- Conte, V.; Bortolini, O.; Carraro, M.; Moro, S. *J. Inorg. Biochem.* **2000**, *80*, 41.
- Bortolini, O.; Conte, V.; Di Furia, F.; Moro, S. *Eur. J. Inorg. Chem.* **1998**, 1193.
- Bortolini, O.; Carraro, M.; Conte, V.; Moro, S. *Eur. J. Inorg. Chem.* **2003**, 42.

vanadium haloperoxidases to catalyze the oxidation of bromide and the bromination of various organic substrates. Although the active site of some haloperoxidases is a monoperoxovanadate moiety to which **His496** covalently binds by its ϵ -N,^{1,2} there is obvious correspondence between diperoxovanadates containing histidine-like ligands^{11–15} and the active site because both of them have one imidazole ring and one peroxide group. Detailed and thorough potentiometric and ⁵¹V NMR spectroscopic investigations of H⁺/H₂-VO₄⁻/H₂O₂/ligand systems have been performed by Pettersson and co-workers.^{16–20} The ligands studied include imidazole, L- α -alanyl-L-histidine, L- α -alanyl-L-serine, picolinic acid, and L-(+)-lactic acid. All these diperoxovanadate complexes were found to be stable under near-physiological conditions, which provided a good starting point to study the interactions between diperoxovanadate complexes [OV(O₂)₂L]ⁿ⁻ ($n=1$ or 3, L = oxalate or H₂O) and a series of histidine-like ligands in solution to simulate the vanadium binding to protein or protein fragments in the active site of the enzyme.

Conte and co-workers have used the NH₄VO₃/H₂O₂/histidine-like ligand systems as models to imitate the active site of haloperoxidases.^{21,22} In a recent mini-review,²² they showed that association of ⁵¹V NMR with electrospray ionization-mass spectrometry (ESI-MS) and density functional calculations is a powerful tool to exploit the solution structures of peroxidic compounds. They concluded that, despite all the efforts made until now,^{8–10,21–24} the complicated structures and chemical behaviors of vanadates in solution are still questions ‘inadequately answered’.²²

In this work, we perform a combination study of NMR and theoretical calculations on the diperoxovanadate complexes [OV(O₂)₂L]ⁿ⁻ ($n=1$ or 3, L = oxalate or H₂O) and a series of histidine-like ligands [imidazole, 2-methylimidazole, 4-methylimidazole, histidine, and carnosine (abbr. Imi, 2-Me-Imi, 4-Me-Imi, His, and Carns, respectively)] in solution. As the NMR signals of the species [OV(O₂)₂L]ⁿ⁻ are clean and simple, the interaction systems are suitable for the study of multinuclear (¹H, ¹³C, and ⁵¹V) NMR, 2D diffusion ordered spectroscopy (DOSY), and variable-temperature ⁵¹V NMR. Some direct NMR data are given for the first time. Theoretical calculations are performed to elucidate the experimental observations. As an improvement upon the previous gas-phase calculations, solvation effects have been taken into account through the polarizable continuum model (PCM). Our study confirms that, through the combination of these methods, structures of all species in the model systems can be obtained and a better understanding of the experimental phenomena can be achieved. We believe that our present results on [OV(O₂)₂L]ⁿ⁻ should be useful for the understanding of the chemistry of vanadium-containing enzymes.

2. Experimental and Theoretical

Materials and Preparation. The diperoxovanadate complex K₃-[OV(O₂)₂(oxa)]·H₂O was prepared according to the literature.²⁵ The ionic medium mimicking the ionic strength of human blood, 0.15

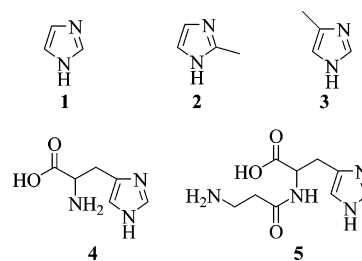


Figure 1. Structures of the histidine-like ligands. **1**, Imi; **2**, 2-Me-Imi; **3**, 4-Me-Imi; **4**, His; **5**, Carns.

mol/L NaCl, D₂O solution^{13–20} at 25 °C, was adopted in all ¹H, ¹³C, and ⁵¹V NMR experiments. The histidine-like ligands (Imi, 2-Me-Imi, 4-Me-Imi, His, and Carns) are all commercial products. Their structures are illustrated in Figure 1. The species [OV(O₂)₂(H₂O)]⁻ was prepared by mixing NH₄VO₃ and H₂O₂.

NMR Spectroscopies. All NMR spectra were recorded on a Varian Unity plus 500 spectrometer operating at 500.4 MHz for ¹H, 125.7 MHz for ¹³C, and 131.4 MHz for ⁵¹V NMR. DSS [3-(trimethylsilyl)-propanesulfonic acid sodium salt] was used as an internal reference for ¹H and ¹³C chemical shifts. ⁵¹V chemical shifts were measured relative to the external standard VOCl₃ with upfield shift being considered as negative. Signal-to-noise ratios were improved by a line-broadening factor of 10 Hz in the Fourier transformation of all ⁵¹V spectra. DOSY (diffusion ordered spectroscopy) was recorded by using a z -gradient probe, which delivers a maximum gradient strength of 30 G/cm. BPPSTE (bipolar pulse pair stimulated echo)²⁶ was used to acquire DOSY spectra. The typical experimental parameters for a 2D ¹H DOSY spectrum are as follows: gradient duration $\delta = 2$ ms, diffusion delay $\Delta = 400$ ms, and time interval between $\pi/2$ and π pulses $\tau = 1.3$ ms. The diffusion coefficient in NMR was generally achieved by stepwise ramping up of the amplitudes of pulsed field gradients, and the diffusion time was optimized for every experiment. The typical time required for a 2D ¹H DOSY spectrum was approximately 0.8 h (16 scans, relaxation delay 4 s).

Computational Method. All quantum mechanics (QM) computations were performed using the B3LYP hybrid density functional, which includes a mixture of Hartree–Fock exchange with Becke88 exchange functional under generalized gradient approximation plus a mixture of Vosko–Wilk–Nusair local correlation functional and Lee–Yang–Parr nonlocal correlation functional.^{27–29} The B3LYP method generally provides good descriptions of reaction profiles, including geometries, heats of reactions, and barrier heights.³⁰

We use the Wadt and Hay core–valence effective core potential³¹ for the metal center (13 explicit electrons for neutral V) with the valence double- ζ contraction of the basis functions (denoted as Lan12dz in Gaussian³²). For O, N, C, and H, we use the standard 6-31+G* basis sets developed by Pople and co-workers.³³ In all calculations, we used the 5d basis sets.

All calculations used the PCM model^{34,35} to describe the effect of solvent. In this approximation, the cavity is created via a series of overlapping spheres. At each self-consistent field (SCF) step,

(26) Stamps, J. P.; Ottink, B.; Visser, J. M.; van Duynhoven, J. P. M.; Hulst, R. *J. Magn. Reson.* **2001**, *151*, 28.

(27) Becke, A. D. *J. Chem. Phys.* **1993**, *98*, 5648.

(28) Lee, C.; Yang, W.; Parr, R. G. *Phys. Rev. B* **1988**, *37*, 785.

(29) Vosco, S. H.; Wilk, L.; Nusair, M. *Can. J. Phys.* **1980**, *58*, 1200.

(30) Baker, J.; Muir, M.; Andzelm, J.; Scheiner, A. In *Chemical Applications of Density-Functional Theory*; Laird, B. B., Ross, R. B., Ziegler, T., Eds.; ACS Symp. Ser. 629; American Chemical Society: Washington, DC, 1996.

(31) Hay P. J.; Wadt, W. R. *J. Chem. Phys.* **1985**, *82*, 299.

(25) Drew, R. E.; Einstein, F. W. B. *Inorg. Chem.* **1972**, *11*, 1079.

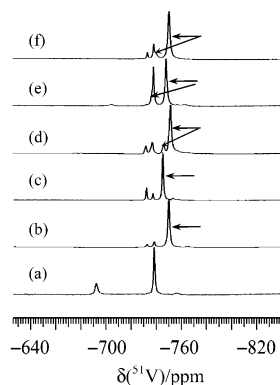


Figure 2. The ^{51}V NMR spectra of the interaction systems between $[\text{OV}(\text{O}_2)_2(\text{oxa})]^{3-}$ and histidine-like ligands with a 1:1 molar ratio in NaCl (0.15 mol/L) D_2O solution. (a) $[\text{OV}(\text{O}_2)_2(\text{oxa})]^{3-}$, (b) $[\text{OV}(\text{O}_2)_2(\text{oxa})]^{3-} + \text{Imi}$, (c) $[\text{OV}(\text{O}_2)_2(\text{oxa})]^{3-} + 2\text{-Me-Imi}$, (d) $[\text{OV}(\text{O}_2)_2(\text{oxa})]^{3-} + 4\text{-Me-Imi}$, (e) $[\text{OV}(\text{O}_2)_2(\text{oxa})]^{3-} + \text{His}$, (f) $[\text{OV}(\text{O}_2)_2(\text{oxa})]^{3-} + \text{Carns}$. The pH values of the systems (b)–(f) are 7.9, 8.3, 7.7, 7.2, and 7.7, respectively. The total concentration of vanadate species is 0.2 mol/L. The peaks of newly formed species $[\text{OV}(\text{O}_2)_2\text{L}]^-$ (L = histidine-like ligand) are indicated by arrows.

we calculated the reaction field in the solvent due to the electrostatic field of the solute wave function. This reaction field was then included in the Fock operator (Kohn–Sham Hamiltonian) to calculate the orbitals of the density functional wave function of the solute. This calculation used a numerical grid to describe the solvent region of space. For a fixed geometry, this process was continued until it was self-consistent. The total energy then included the QM energy (which includes rearrangement effects due to the solvent) and the solute–solvent interactions. The forces on the QM atoms due to the solvent are also calculated so that the geometry could be calculated in the presence of the solvent. However, in this work, the single-point solvation (free) energy was calculated at each optimized gas-phase geometry.

All calculations were carried out with the Gaussian 98 program suite.³² Vibrational frequencies were calculated to ensure that each minimum in the gas phase is a true local minimum (only real frequencies). All energies reported in this work are $\Delta G(298\text{ K})$ in kcal/mol.

3. Results and Discussion

3.1. ^{51}V NMR Spectra of the Interaction Systems. As shown in Figure 2a, the ^{51}V NMR spectrum of the $[\text{OV}(\text{O}_2)_2(\text{C}_2\text{O}_4)]^{3-}$ solution has a large peak at -738 ppm and a small peak at -692 ppm. According to the previous reports, the peak at -738 ppm is assigned to $[\text{OV}(\text{O}_2)_2(\text{C}_2\text{O}_4)]^{3-}$.^{36,37} The peak locating at -692 ppm is assigned to $[\text{OV}(\text{O}_2)_2(\text{D}_2\text{O})]^-$.^{36,38} When 1 equiv of a histidine-like ligand (L = Imi, 2-Me-

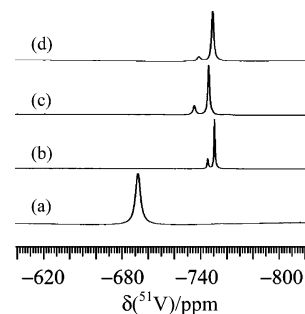


Figure 3. The ^{51}V NMR spectra of the interaction systems $\text{NH}_4\text{VO}_3/\text{H}_2\text{O}_2/\text{ligand}$ with a 1:5:2 molar ratio in NaCl (0.15 mol/L) D_2O solution. (a) $[\text{OV}(\text{O}_2)_2(\text{H}_2\text{O})]^-$, (b) $[\text{OV}(\text{O}_2)_2(\text{H}_2\text{O})]^- + 4\text{-Me-Imi}$, (c) $[\text{OV}(\text{O}_2)_2(\text{H}_2\text{O})]^- + \text{His}$, (d) $[\text{OV}(\text{O}_2)_2(\text{H}_2\text{O})]^- + \text{Carns}$. The pH values of the systems (b)–(d) are 8.4, 7.3, and 7.8, respectively. The total concentration of vanadate species is 0.2 mol/L.

Imi, 4-Me-Imi, His, and Carns, respectively) is added to the $[\text{OV}(\text{O}_2)_2(\text{C}_2\text{O}_4)]^{3-}$ solution, the area of the $[\text{OV}(\text{O}_2)_2(\text{C}_2\text{O}_4)]^{3-}$ peak decreases and new peaks appear. The new peaks at about -750 (Imi), -746 (2-Me-Imi), -747 and -753 (4-Me-Imi), -738 and -748 (His), and -738 and -748 (Carns) ppm are assigned to six-coordinative species $[\text{OV}(\text{O}_2)_2\text{L}]^-$ (L = histidine-like ligands).^{11–15,17,22,39–41} Note that the chemical shift of the species $[\text{OV}(\text{O}_2)_2(\text{Carns})]^-$ is reported here for the first time. The intensities of the new peaks increase with the increasing quantity of ligand. The small new peak at -732 ppm is assigned to $[\text{V}(\text{O}_2)_3]^-$.⁴¹ The peaks at -757 ppm in Figure 2a and c and at -763 ppm in Figure 2b are assigned to $\{[\text{OV}(\text{O}_2)_2]_2\}^{2-}$ ⁴¹ and $\{[\text{OV}(\text{O}_2)_2]_2(\text{OD})\}^{3-}$,⁴² respectively.

There are two peaks for species $[\text{OV}(\text{O}_2)_2\text{L}']^-$ (L' = 4-Me-Imi, His, and Carns) in ^{51}V spectra of the interaction systems; some peaks of the newly formed complexes overlap with the peak of -738 ppm arising from $[\text{OV}(\text{O}_2)_2(\text{C}_2\text{O}_4)]^{3-}$. To make a clear assignment, the interaction systems between $[\text{OV}(\text{O}_2)_2(\text{H}_2\text{O})]^-$ and 4-Me-Imi, His, and Carns prepared under the condition of $\text{NH}_4\text{VO}_3/\text{H}_2\text{O}_2/\text{ligands}$ (1:5:2 molar ratio) were studied for comparison. The results confirm that there is a peak at around -738 ppm in the systems of $\text{NH}_4\text{VO}_3/\text{H}_2\text{O}_2/\text{His}$ and $\text{NH}_4\text{VO}_3/\text{H}_2\text{O}_2/\text{Carns}$, close to the location of the $[\text{OV}(\text{O}_2)_2(\text{oxa})]^{3-}$ peak (Figure 3). Comparing the relative areas of the peroxovanadate species in Figures 2 and 3, we conclude that the order of the reactivity of the ligands to the peroxovanadate species is $\text{Imi} > 2\text{-Me-Imi} > \text{Carns} \approx 4\text{-Me-Imi} > \text{His}$.

The fact that there exist two peaks for the species $[\text{OV}(\text{O}_2)_2\text{L}']^-$ (L' = 4-Me-Imi, His, and Carns) in the ^{51}V NMR spectra indicates that there are two types of coordination for these ligands binding to the metal center. Because of the higher coordination ability of the imidazole N atoms

- (32) Frisch, M. J.; Trucks, G. W.; Schlegel, H. B.; Scuseria, G. E.; Robb, M. A.; Cheeseman, J. R.; Zakrzewski, V. G.; Montgomery, J. A., Jr.; Stratmann, R. E.; Burant, J. C.; Dapprich, S.; Millam, J. M.; Daniels, A. D.; Kudin, K. N.; Strain, M. C.; Farkas, O.; Tomasi, J.; Barone, V.; Cossi, M.; Cammi, R.; Mennucci, B.; Pomelli, C.; Adamo, C.; Clifford, S.; Ochterski, J.; Petersson, G. A.; Ayala, P. Y.; Cui, Q.; Morokuma, K.; Malick, D. K.; Rabuck, A. D.; Raghavachari, K.; Foresman, J. B.; Cioslowski, J.; Ortiz, J. V.; Stefanov, B. B.; Liu, G.; Liashenko, A.; Piskorz, P.; Komaromi, I.; Gomperts, R.; Martin, R. L.; Fox, D. J.; Keith, T.; Al-Laham, M. A.; Peng, C. Y.; Nanayakkara, A.; Gonzalez, C.; Challacombe, M.; Gill, P. M. W.; Johnson, B. G.; Chen, W.; Wong, M. W.; Andres, J. L.; Head-Gordon, M.; Replogle, E. S.; Pople, J. A. *Gaussian 98*; Gaussian, Inc.: Pittsburgh, PA, 1998.
- (33) Hariharan, P. C.; Pople, J. A. *Chem. Phys. Lett.* **1972**, *16*, 217.
- (34) Miertus, S.; Scrocco, E.; Tomasi, J. *Chem. Phys.* **1981**, *55*, 117.
- (35) Barone, V.; Cossi, M.; Tomasi, J. *J. Chem. Phys.* **1997**, *107*, 3210.

- (36) Zhou, X. W.; Ye, J. L.; Chen, Z.; Chen, Z. W.; Yu, L. J.; Huang, P. Q.; Wu, Q. Y. *Chin. J. Struct. Chem.* **2000**, *19*, 343.
- (37) Ballistreri, F. P.; Barbuzzi, E. G. M.; Tomaselli, G. A.; Toscano, R. M. *J. Inorg. Biochem.* **2000**, *80*, 173.
- (38) Buhl, M.; Parrinello, M. *Chem. Eur. J.* **2001**, *7*, 4487.
- (39) Keramidias, A. D.; Miller, S. M.; Anderson, O. P.; Crans, D. C. *J. Am. Chem. Soc.* **1997**, *119*, 8901.
- (40) Tracey, A. S.; Jaswal, J. S. *J. Am. Chem. Soc.* **1992**, *114*, 3835.
- (41) Tracey, A. S.; Jaswal, J. S. *Inorg. Chem.* **1993**, *32*, 4235.
- (42) Harrison, A. T.; Howarth, O. W. *J. Chem. Soc., Dalton Trans.* **1985**, 1173.

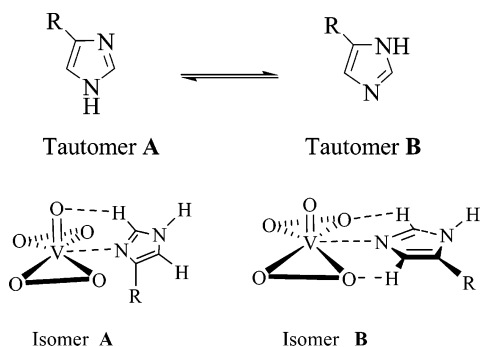


Figure 4. The tautomers of 4-Me-Imi, His, and Carns and the resulting isomers when they coordinate to vanadium atom, where R = substituent group.

Table 1. Changes of Molar Ratios of Isomers **A** and **B** with the Variation of Temperature in $\text{NH}_4\text{VO}_3/\text{H}_2\text{O}_2/\text{Ligand}$ Systems with a 1:5:2 Molar Ratio^a

| T/°C | A:B | | |
|------|--------------|---------|-----------|
| | L = 4-Me-Imi | L = His | L = Carns |
| 25 | 1:4.5 | 1:5.2 | 1:16.1 |
| 40 | 1:4.4 | 1:4.8 | 1:13.7 |
| 55 | 1:4.2 | 1:4.6 | 1:10.6 |
| 70 | 1:3.9 | 1:4.5 | 1:9.5 |

^a The pH values of different interaction systems are 8.4, 7.2, and 7.8 for 4-Me-Imi, His, and Carns, respectively, at 25 °C. The ionic medium is 0.15 mol/L NaCl in D_2O solution at 25 °C, mimicking the ionic strength of human blood. The total concentration of vanadate species is 0.2 mol/L.

than that of N atoms in the other groups such as terminal amino, it is the imidazole N that coordinates to the vanadium atom for the histidine-like ligands. As we know, tautomerism exists in the D_2O solution of free histidine-like ligands studied herein. Since the two nitrogen atoms in the imidazole ring of 4-Me-Imi, His, and Carns are not equivalent due to the position of the substituent group, R, the tautomerism of each ligand results in two tautomers (see Figure 4, tautomers **A** and **B**). When they coordinate to the vanadium atom, two $[\text{OV}(\text{O}_2)_2\text{L}]^-$ isomers form (see Figure 4, isomers **A** and **B**). Here, isomer **B** is the major product.^{13,43} The ratio between isomers **A** and **B** is influenced by several factors such as the pH value⁴³ and the properties of the medium.

Variable-temperature technology was employed to study the influence of temperature on the equilibria of the interaction systems of $\text{NH}_4\text{VO}_3/\text{H}_2\text{O}_2/\text{ligand}$ (1:5:2 molar ratio, ligand = 4-Me-Imi, His, or Carns) within the range of 25–70 °C. Table 1 lists the variation of molar ratios of isomers **A** and **B** with temperature. On the basis of the results of variable-temperature ^{51}V NMR spectra, the following conclusions can be drawn. (1) The quantity of isomer **B** decreases and that of **A** increases when the temperature increases. Data from ^1H and ^{13}C NMR (See next section) infer that isomers **A** and **B** cannot be converted into each other directly. Generally, the ligand first dissociates from an isomer, and then re-coordinates to vanadium to form isomer **A** or **B** (the higher the temperature, the more isomer **A**). (2) All peroxovanadate species are stable within the experimental temperature range.

3.2. ^1H and ^{13}C NMR Spectra of the Interaction Systems. The ^1H and ^{13}C NMR spectra of the interaction systems of $[\text{OV}(\text{O}_2)_2(\text{oxa})]^{3-}$ and ligands were recorded. The assignments are listed in Table 2.

When the ligands are Imi and 2-Me-Imi, there are two groups of peaks related to the ligands in ^1H and ^{13}C NMR spectra of the interaction systems, respectively. One is assigned to the free ligand and the other to the coordination ligand belonging to the newly formed species. When the ligands are 4-Me-Imi, His, and Carns, both ^1H and ^{13}C NMR spectra have three groups of peaks. One is assigned to the free ligands and the other two are assigned to the coordination ligands in form of isomers **A** and **B**, respectively. Unlike the previous study,⁴³ the NMR peaks from the imidazole ring of the free ligand are narrow.

When the ligands are His and Carns, the 1D ^1H NMR spectra of the interaction systems are so complicated that 2D NMR technology was used for an unambiguous assignment. With the help of ^1H – ^1H COSY and ^{13}C NMR spectra, we can successfully assign ^1H NMR signals of the interaction system between $[\text{OV}(\text{O}_2)_2(\text{oxa})]^{3-}$ and His with a 1:1 molar ratio. However, when the ligand is changed to Carns, the signals of isomer **A** are very weak and the signal-to-noise ratio of ^{13}C NMR spectrum is poor. Therefore, we increased the amount of Carns to get better spectra. Figure 5 shows the ^{13}C NMR spectra of the interaction system between $[\text{OV}(\text{O}_2)_2(\text{oxa})]^{3-}$ and Carns with a 1:2 molar ratio in imidazole ring. The signals of isomer **A** are rather weak. Other signals are listed in Table 2. Figure 6 is the ^1H – ^1H COSY spectra of the same system described above. There are three groups of signals in Figure 6. The cross-peaks at 7.05, 7.24, and 7.27 ppm come from the coupling of two hydrogen atoms in the imidazole ring. The assignments of other signals located in the interval from 2.68 to 4.56 ppm are also listed in Table 2.

The molar ratio of isomers **A** and **B** is calculated to be 1:16.1 from the ^{51}V NMR spectrum of the $\text{NH}_4\text{VO}_3/\text{H}_2\text{O}_2/\text{Carns}$ (1:5:2 molar ratio) system at 25 °C. This may be the reason that earlier studies often missed isomer **A** and only reported isomer **B**. In ref 44, complexes $\text{NH}_4[\text{OV}(\text{O}_2)_2\text{His}] \cdot \text{H}_2\text{O}$ and $\text{H}[\text{OV}(\text{O}_2)_2\text{His}]$ have been proposed to model the active site of V–BrPO. Their ^{51}V NMR spectra gave three peaks (–690/–692, –737/–737, –747/–748 ppm), implying three groups of signals. This is in agreement with our observation. However, their ^1H and ^{13}C NMR spectra only gave two groups of data, inconsistent with the anticipation based on the ^{51}V NMR spectra. Moreover, the chemical shift of the carboxylic carbon in His has been missed.⁴⁴ Reference 17 only reported ^1H , ^{13}C , and ^{51}V NMR data of free and coordinated Ah (Ah = L- α -Alanyl-L-histidine) in the $\text{H}^+/\text{H}_2\text{VO}_4^-/\text{Ah}$ system where Ah was coordinated to vanadium by its ϵ -N of the imidazole residue. Reference 41 reported two isomers formed from the reaction system between diperoxovanadate and His. Their NMR data are coincident with our measurements.

(43) Jaswal, J. S.; Tracey, A. S. *J. Am. Chem. Soc.* **1993**, *115*, 5600.

(44) Mukherjee, J.; Ganguly, S.; Bhattacharjee, M. *Indian J. Chem. A.* **1996**, *35*, 471.

Table 2. ^1H , ^{13}C , and ^{51}V NMR Spectra of the Interaction Systems between $[\text{OV}(\text{O}_2)_2(\text{oxa})]^{3-}$ and Histidine-like Ligands^a

| ligands | species | chemical shifts | | |
|-------------------|---|---|---|-----------------------|
| | | ^1H (ppm) | ^{13}C (ppm) | ^{51}V (ppm) |
| oxa ²⁻ | $[\text{OV}(\text{O}_2)_2(\text{oxa})]^{3-}$ | | 170.5, 175.9 | -738 |
| Imi | $[\text{OV}(\text{O}_2)_2(\text{Imi})]^-$ | 7.41(s, 1H, CH), 7.49(s, 1H, CH), 8.31(s, 1H, CH) | 120.7, 129.0, 139.5 | -750 |
| | Imi | 7.25(s, 2H, CH), 8.08(s, 1H, CH) | 123.3, 137.7 | |
| 2-Me-Imi | $[\text{OV}(\text{O}_2)_2(2\text{-Me-Imi})]^-$ | 2.57(s, 3H, CH ₃), 7.09(s, 1H, CH), 7.21(s, 1H, CH) | 15.4, 119.3, 128.8, 149.8 | -746 |
| | 2-Me-Imi | 2.65(s, 1H, CH ₃), 7.22(s, 2H, CH) | 14.0, 122.3, 147.6 | |
| 4-Me-Imi | $[\text{OV}(\text{O}_2)_2(4\text{-Me-Imi})]^-$ (isomer A) | 2.39(s, 3H, CH ₃), 7.13(s, 1H, CH), 8.01(s, 1H, CH) | 14.3, 117.6, 138.8, 139.1 | -747 |
| | $[\text{OV}(\text{O}_2)_2(4\text{-Me-Imi})]^-$ (isomer B) | 2.33(s, 3H, CH ₃), 7.18(s, 1H, CH), 8.15(s, 1H, CH) | 11.5, 125.8, 131.2, 138.6 | -753 |
| | 4-Me-Imi | 2.30(s, 3H, CH ₃), 7.07(s, 1H, CH), 8.29(s, 1H, CH) | 13.1, 120.0, 135.1, 138.0 | |
| His | $[\text{OV}(\text{O}_2)_2(\text{His})]^-$ (isomerA) | 3.36(m, 1H, CH ₂), 3.63(dd, 1H, $J = 15.56, 5.03$ Hz, CH ₂), 4.16(dd, 1H, $J = 7.33, 5.03$ Hz, CH), 7.34(s, 1H, CH), 8.06(s, 1H, CH) | 30.6, 57.1, 120.1, 136.4, 140.0, 176.3 | -738 |
| | $[\text{OV}(\text{O}_2)_2(\text{His})]^-$ (isomerB) | 3.32(m, 1H, CH ₂), 3.38(m, 1H, CH ₂), 4.06(m, 1H, CH), 7.40(s, 1H, CH), 8.29(s, 1H, CH) | 28.5, 56.4, 128.1, 128.6, 140.3, 175.7 | -748 |
| | His | 3.18(m, 1H, CH ₂), 3.25(m, 1H, CH ₂), 4.02(m, 1H, CH), 7.14(s, 1H, CH), 7.97(s, 1H, CH) | 30.1, 57.0, 119.5, 133.5, 138.3, 176.2 | |
| Carns | $[\text{OV}(\text{O}_2)_2(\text{Carns})]^-$ (isomerA) | 2.68(m, 2H, CH ₂), 3.22(m, 2H, CH ₂), 3.24(m, 2H, CH ₂), 3.46(dd, 1H, $J = 15.56, 3.97$ Hz, CH ₂), 4.56(m, 1H, CH), 7.24(s, 1H, CH), 8.00(s, 1H, CH) | 29.9, 31.6, 34.7, 38.3, 57.9, 118.8, 138.9, 139.3, 174.1, 180.4 | -738 |
| | $[\text{OV}(\text{O}_2)_2(\text{Carns})]^-$ (isomerB) | 2.68(m, 2H, CH ₂), 3.09(dd, 1H, $J = 15.26, 9.85$ Hz, CH ₂), 3.22(m, 2H, CH ₂), 3.31(dd, 1H, $J = 15.26, 3.66$ Hz, CH ₂), 4.54(dd, 1H, $J = 9.85, 3.66$ Hz, CH), 7.27(s, 1H, CH), 8.21(s, 1H, CH) | 29.9, 31.3, 34.7, 38.3, 56.9, 127.3, 131.2, 139.4, 174.1, 179.6 | -748 |
| | Carns | 2.68(m, 2H, CH ₂), 2.98(dd, 1H, $J = 15.11, 9.16$ Hz, CH ₂), 3.14(m, 1H, $J = 15.11, 4.26$ Hz, CH ₂), 3.22(m, 2H, CH ₂), 4.48(dd, 1H, $J = 9.16, 4.26$ Hz, CH), 6.99(s, 1H, CH), 7.79(s, 1H, CH) | 29.9, 31.3, 34.7, 38.3, 57.7, 119.8, 135.5, 138.1, 174.1, 180.4 | |

^a The molar ratio between $[\text{OV}(\text{O}_2)_2(\text{oxa})]^{3-}$ and ligand is 1:1 for Imi, 2-Me-Imi, 4-Me-Imi, or His and is 1:2 for Carns. The pH values of different interaction systems are 7.9, 8.3, 7.7, 7.2, and 8.1 when ligands are Imi, 2-Me-Imi, 4-Me-Imi, His, and Carns, respectively.

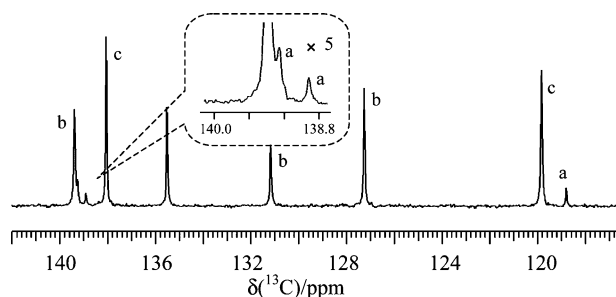


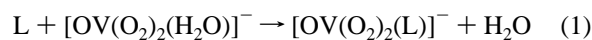
Figure 5. The ^{13}C NMR spectrum of the imidazole ring in the interaction system between $[\text{OV}(\text{O}_2)_2(\text{oxa})]^{3-}$ and Carns with a 1:2 molar ratio in NaCl (0.15 mol/L) D_2O solution. The pH value of the interaction system is 8.1. The total concentration of vanadate species is 0.2 mol/L. a, isomer A; b, isomer B; c, free Carns.

3.3. 2D ^1H DOSY Spectra of the Interaction Systems.

The systems of $[\text{OV}(\text{O}_2)_2(\text{oxa})]^{3-}$ and 4-Me-Imi, His, or Carns with a 1:2 molar ratio in solution were studied by DOSY. In the DOSY spectra, the x-axis shows the chemical

shift, while the y-axis indicates the diffusion coefficient, which is related to the molecular weight and/or molecular configuration. Figure 7 shows the DOSY spectra of the imidazole ring of the interaction systems, where I, II, and III correspond to the ligands of 4-Me-Imi, His, and Carns, respectively. It clearly illustrates the presence of three components. The component with the fastest diffusion rate (indicated by the solid line) is the free ligand. On the basis of the NMR data in Table 2, the component with the faster diffusion rate (indicated by the dash-dotted line) is isomer B; isomer A has the lowest diffusion rate (indicated by the dotted line). Therefore, the 2D DOSY spectra can be used as a supplement to the general ^1H NMR assignment.

3.4. Theoretical Study on the Interaction Systems. We have examined the reactions in solutions:



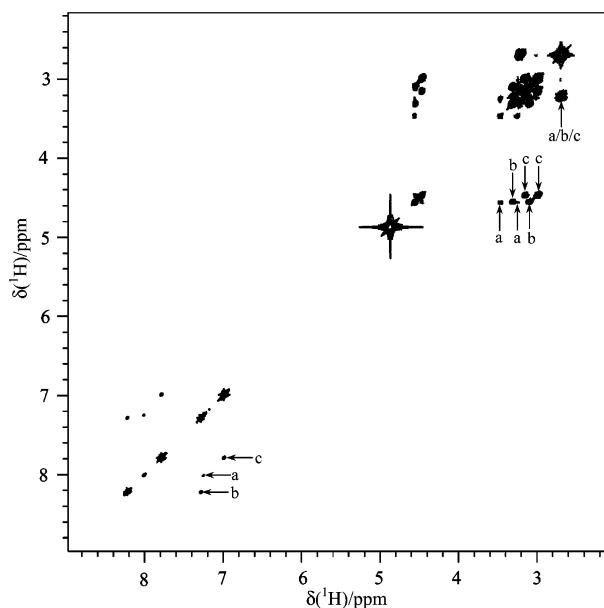


Figure 6. The ^1H - ^1H COSY spectrum of the interaction system between $[\text{OV}(\text{O}_2)_2(\text{oxa})]^{3-}$ and Carns with a 1:2 molar ratio in NaCl (0.15 mol/L) D_2O solution. The pH value of the interaction system is 8.1. The total concentration of vanadate species is 0.2 mol/L. a, isomer A; b, isomer B; c, free Carns.

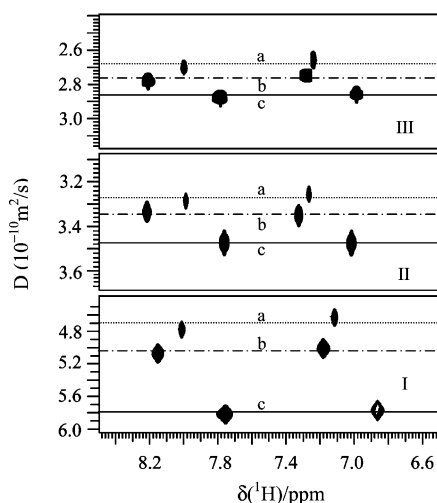


Figure 7. 2D ^1H DOSY spectra of the imidazole ring in the interaction systems between $[\text{OV}(\text{O}_2)_2(\text{oxa})]^{3-}$ and histidine-like ligands with a 1:2 molar ratio in NaCl (0.15 mol/L) D_2O solution. The pH values of the interaction systems are 8.8, 7.6, and 8.1 when the ligands are 4-Me-Imi (I), His (II), and Carns (III), respectively. The total concentration of vanadate species is 0.2 mol/L. a, isomer A; b, isomer B; c, free ligands.

For free histidine-like ligands such as 4-Me-Imi, His, and Carns, there are two tautomers which differ in the position of the substituent group with respect to the imidazole N atom (Figure 4). This leads to two reaction routes, **Route A** and **Route B**, in the interaction systems between $[\text{OV}(\text{O}_2)_2(\text{H}_2\text{O})]^-$ and histidine-like ligands, as shown in Figure 8.

Tables 3 and 4 summarize the geometric parameters of the optimized interaction systems. In the $[\text{OV}(\text{O}_2)_2(\text{H}_2\text{O})]^-$ system, one O-H bond of water is parallel to the $\text{V}=\text{O}_1$ bond while the other O-H bond of water is perpendicular to the $\text{V}=\text{O}_1$ bond (or parallel to the $\text{V}-\text{O}_2$ bond) such that the dihedral angles are $\text{H}_1-\text{O}_1-\text{V}-\text{O} = 1.3^\circ$ and $\text{H}_2-\text{O}_2-\text{V}-\text{O} = -5.4^\circ$. As compared to the free $[\text{OV}(\text{O}_2)_2]^-$, $\text{V}=\text{O}_1$

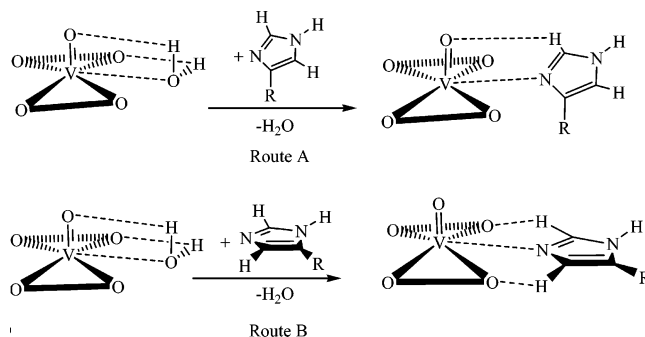
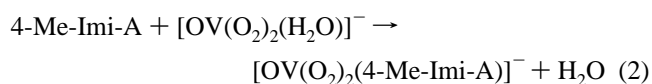


Figure 8. Reactions of the interaction systems.

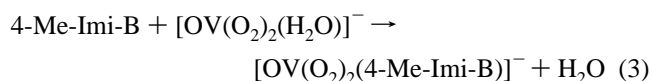
O_1 and $\text{V}-\text{O}_2$ are elongated by 0.017 and 0.026 Å, respectively, upon forming hydrogen bonds with water. The hydrogen-bond lengths are $\text{O}_1-\text{H}_1 = 2.112$ Å and $\text{O}_2-\text{H}_2 = 2.179$ Å. The $\text{V}-\text{O}$ distance is 2.308 Å.

In the active site of chloroperoxidase from the fungus *Curvularia inaequaliz*, **His496** coordinates to vanadate(V) by its $\epsilon\text{-N}$.^{1,2} For all histidine-like ligands studied here, we find that ligands bind to the metal by using the same $\epsilon\text{-N}$. The $\text{V}-\text{N}$ bond distances are 2.20 and 2.18 Å for isomers **A** and **B**, respectively. Most interestingly, we find that the plane of the imidazole ring is parallel to the $\text{V}=\text{O}_1$ bond in isomer **A**, while that of the imidazole ring is perpendicular to the $\text{V}=\text{O}_1$ bond in isomer **B**. Thus, O_1-H is around 2.46 Å in isomer **A** and $\text{O}_2-\text{H}/\text{O}_4-\text{H}$ are around 2.35/2.55 Å in isomer **B**. Dihedral angles experience a large variation for different ligands. On going from 4-Me-Imi to His and then to Carns, the dihedral angle of $\text{H}-\text{O}_1-\text{V}-\text{N}$ in isomer **A** increases from 0.7° to 3.8° and then to 8.9° , diverging from the ideal 0° to an increased degree as the size of the R group is increased. Similarly, on going from 4-Me-Imi to His and then to Carns, the dihedral angle of $\text{H}-\text{O}_2-\text{V}-\text{N}$ in isomer **B** increases from -18.0° to -21.9° and then to -27.2° .

The reactivity of ligand L depends on a combined effect of the intrinsic binding strength between $[\text{OV}(\text{O}_2)_2]^-$ and L in $[\text{OV}(\text{O}_2)_2(\text{L})]^-$ and the solvation energy difference between $[\text{OV}(\text{O}_2)_2(\text{L})]^-$ and L. For the free ligand of 4-Me-Imi in the gas phase, we find that tautomer **A** (4-Me-Imi-A, for short) is 0.53 kcal/mol more stable than tautomer **B** (4-Me-Imi-B). Solvation energies compensate this difference, being -5.55 kcal/mol for 4-Me-Imi-A and -5.84 kcal/mol for 4-Me-Imi-B. For $\text{L} = 4\text{-Me-Imi}$ in $[\text{OV}(\text{O}_2)_2(\text{L})]^-$, we find that $[\text{OV}(\text{O}_2)_2(4\text{-Me-Imi-A})]^-$ is 0.81 kcal/mol more stable than $[\text{OV}(\text{O}_2)_2(4\text{-Me-Imi-B})]^-$ in the gas phase. Solvation effects again reverse this order of stability. Solvation energies for $[\text{OV}(\text{O}_2)_2(4\text{-Me-Imi-A})]^-$ and $[\text{OV}(\text{O}_2)_2(4\text{-Me-Imi-B})]^-$ are -68.17 and -70.31 kcal/mol, respectively. Thus, we have



$$\Delta G (298 \text{ K}) = 1.8 \text{ (in vacuo) and } -11.0 \text{ (in solution);}$$



$$\Delta G (298 \text{ K}) = 2.1 \text{ (in vacuo) and } -12.6 \text{ (in solution).}$$

Table 3. Optimized Geometric Data for $[\text{OV}(\text{O}_2)_2]^-$ in Various Coordination States

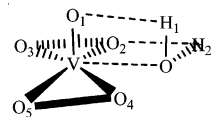
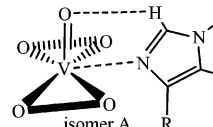
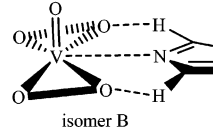
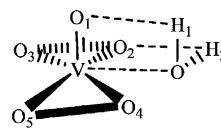
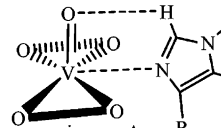
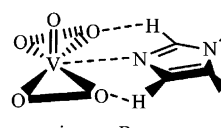
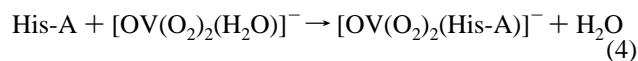
| Ligands | V=O ₁ | V-O ₂ | V-O ₃ | O ₂ -O ₃ | O ₂ -V-O ₄ | O ₃ -V-O ₅ |
|---|------------------|------------------|------------------|--------------------------------|----------------------------------|----------------------------------|
|  | - | 1.604 | 1.816 | 1.868 | 1.460 | 129.3 |
| H ₂ O | 1.621 | 1.842 | 1.876 | 1.450 | 131.5 | 91.4 |
|  | 4-Me-Imi | 1.616 | 1.850 | 1.882 | 1.449 | 131.6 |
| His | 1.615 | 1.848 | 1.881 | 1.449 | 131.3 | 90.4 |
| Carns | 1.614 | 1.847 | 1.881 | 1.449 | 131.1 | 90.6 |
|  | 4-Me-Imi | 1.607 | 1.865 | 1.883 | 1.448 | 133.8 |
| His | 1.606 | 1.865 | 1.884 | 1.448 | 133.9 | 91.2 |
| Carns | 1.606 | 1.865 | 1.882 | 1.448 | 133.8 | 91.2 |

Table 4. Optimized Geometric Data for the Interaction between $[\text{OV}(\text{O}_2)_2]^-$ and Various Ligands

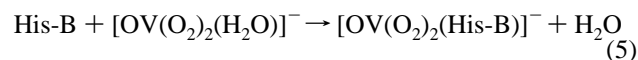
| Ligands | V-O/N | O ₁ -H | O _{2/4} -H | H-O ₁ -V-O/N | H-O _{2/4} -V-O/N | |
|---|------------------|-------------------|---------------------|-------------------------|---------------------------|-------------------|
|  | H ₂ O | <u>2.308</u> | <u>2.112</u> | <u>2.179</u> | <u>1.3</u> | <u>-5.4</u> |
|  | 4-Me-Imi | <u>2.201</u> | <u>2.463</u> | - | <u>0.7</u> | <u>131.6</u> |
| His | <u>2.203</u> | <u>2.461</u> | - | <u>3.8</u> | <u>131.3</u> | |
| Carns | <u>2.200</u> | <u>2/467</u> | - | <u>8.9</u> | <u>131.1</u> | |
|  | 4-Me-Imi | <u>2.181</u> | - | <u>2.358/2.515</u> | - | <u>-18.0/19.7</u> |
| His | <u>2.187</u> | - | <u>2.349/2.557</u> | - | <u>-21.9/21.6</u> | |
| Carns | <u>2.183</u> | - | <u>2.355/2.592</u> | - | <u>-32.3/32.0</u> | |

Hence, our calculations show that solvation effects play a key role here. While replacing H₂O in $[\text{OV}(\text{O}_2)_2(\text{H}_2\text{O})]^-$ with 4-Me-Imi is an unfavorable process in the gas phase, it is thermodynamic favorable in the solution phase. It is mainly due to the difference in the solvation energies of $[\text{OV}(\text{O}_2)_2(4\text{-Me-Imi-A})]^-$ and $[\text{OV}(\text{O}_2)_2(4\text{-Me-Imi-B})]^-$ that isomer **B** outweighs isomer **A**, as observed in the experiments.

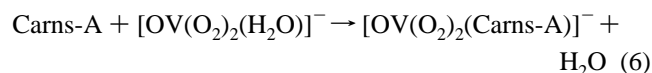
Similar calculations were also performed for ligands of His and Carns.



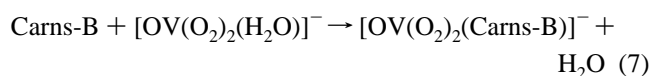
$\Delta G(298 \text{ K}) = 1.5$ (in vacuo) and -8.8 (in solution);



$\Delta G(298 \text{ K}) = 3.6$ (in vacuo) and -11.4 (in solution).



$\Delta G(298 \text{ K}) = 2.3$ (in vacuo) and -5.6 (in solution);



$\Delta G(298 \text{ K}) = 0.2$ (in vacuo) and -12.1 (in solution).

As compared to reaction 3, replacing H₂O in $[\text{OV}(\text{O}_2)_2(\text{H}_2\text{O})]^-$ with His (reaction) is less favorable than replacing H₂O in $[\text{OV}(\text{O}_2)_2(\text{H}_2\text{O})]^-$ with 4-Me-Imi, while replacing H₂O in $[\text{OV}(\text{O}_2)_2(\text{H}_2\text{O})]^-$ with Carns (reaction) is comparable to replacing H₂O in $[\text{OV}(\text{O}_2)_2(\text{H}_2\text{O})]^-$ with 4-Me-Imi. This is in accordance with the experimental fact that the reactivity of the ligands to peroxovanadate species is Carns \approx 4-Me-Imi $>$ His. While calculations predict that reaction 3 is 1.6 kcal/mol more favorable than reaction 2, reaction 5 is 2.6 kcal/mol more favorable than reaction 4 and reaction 7 is 6.5 kcal/mol more favorable than reaction 6; the experiments show that the molar ratio between isomers **A** and **B** is 1: 4.5 for 4-Me-Imi; 1:5.2 for His; and 1:16.1. Thus, theory and experiment reach a qualitative agreement.

4. Conclusions

Several NMR experimental techniques together with density functional calculations have been employed to study the interaction systems between $[\text{OV}(\text{O}_2)_2(\text{oxa})]^{3-}$ and the histidine-like ligands. In 0.15 mol/L NaCl, D₂O solution,

there are competitive coordination interactions between $[\text{OV}(\text{O}_2)_2(\text{oxa})]^{3-}$ and the histidine-like ligands. NMR experiments show that the coordination capability among the ligands is $\text{Imi} > 2\text{-Me-Imi} > \text{Carns} \approx 4\text{-Me-Imi} > \text{His}$. When ligands are 4-Me-Imi, His, and Carns, a pair of isomers has been observed. Theoretical calculations show that it is the solvation effect that stabilizes one isomer over the other. We believe that our present results on $[\text{OV}(\text{O}_2)_2\text{L}]^{n-}$ should be useful for the understanding of the chemistry of a vanadium-containing enzyme.

Acknowledgment. This work was supported by National Natural Science Foundation of China (10234070, 10104011, and 20021002), National Natural Science Foundation of Fujian (2002F010), the Ministry of Science and Technology of China (2004CB719902, 2001CB610506), TRAPOYT from the Ministry of Education of China, and State Key Laboratory of Physical Chemistry of Solid Surface of China.

IC050739F